Anomalous Propagation Loss in Photonic Crystal Waveguides

Zhi-Yuan Li[1,2,*] and Kai-Ming Ho[1]

[1]*Ames Laboratory and Department of Physics and Astronomy, Iowa State University, Ames, Iowa 50011, USA*
[2]*Institute of Physics, Chinese Academy of Sciences, P.O. Box 603, Beijing 100080, China*

(Received 11 August 2003; published 12 February 2004)

Propagation loss can occur in photonic crystal waveguides without complete optical confinement. We employ a highly efficient transfer-matrix method which allows for accurate and reliable extraction of the propagation loss even at an extremely low level. The results for a two-dimensional photonic crystal waveguide shows that the loss exponentially decays via the waveguide wall thickness. An anomalous phenomenon is found where the loss for guided modes near the upper band gap edge can be several orders of magnitude smaller than that for modes in the middle of the band gap. This anomaly can be well explained by the localization degree of guided modes at different frequency domains.

DOI: 10.1103/PhysRevLett.92.063904 PACS numbers: 42.70.Qs, 41.20.Jb, 78.70.Gq

In recent years photonic crystal (PC) waveguides have attracted extensive interest in the hope of building an ultrasmall optical integrated circuit on the platform of photonic crystals [1–7]. A PC waveguide can efficiently manipulate the propagation of electromagnetic (EM) waves at subwavelength sizes. Lossless propagation of EM waves can be realized in ideal PC waveguides either through photonic band gap (PBG) effects in pure two-dimensional (2D) or 3D crystals [1–3] or through hybrid mechanisms of the PBG and index guiding in a 2D PC slab waveguide [4–7]. However, propagation loss always occurs in a realistic PC waveguide, leading to exponential decay of wave when it travels, either because of limited cladding wall thickness or because of scattering by nonuniformity and roughness [4–8]. There have been many experimental [4–7] and theoretical [9–14] efforts to measure, evaluate, and understand the propagation loss in a realistic PC waveguide, in a hope to find ways to reduce the propagation loss to a level as low as possible.

In principle, the propagation loss should be monitored in real space by looking at the decay pattern of EM fields along the waveguide. In experiment, this can be done by changing the length of a PC waveguide and recording the output power [4–7]. In theory, one can adopt a fixed-length waveguide and see how an input wave decays when it travels along the channel. If the propagation loss is weak, a very long waveguide is necessary to extract a reliable value of decay constant, and this results in a serious numerical burden since it is proportional to the waveguide length. For this reason, only waveguides with a relatively high loss have been studied by rigorous 3D numerical simulations [5,14]. To relieve this theoretical difficulty, other indirect schemes are adopted, such as the time-domain damping techniques [9,10], coupled-mode theory [11], and perturbation techniques [12,13]. In most of these approaches, the true decay constant β for a guided mode is calculated approximately by relating it with the time-domain damping factor for a unperturbed lossless guided mode through the group velocity of the guided mode.

In this Letter we employ a highly efficient plane-wave based transfer-matrix method (TMM) [15,16] to directly solve the decay constant β for a guided wave traveling along a PC waveguide. The numerical burden of this approach does not depend on the waveguide length, and therefore can efficiently handle PC waveguides with low propagation loss. A supercell is adopted to describe the quasi-1D PC waveguide. In order to account for realistic wave leakage in a lossy waveguide, perfect absorption layers (PALs) are placed at the boundaries of the supercell, so that all waves impinging on the boundaries are nearly 100% absorbed, and no cross talk between adjacent supercells can occur. Figure 1 displays the geometry of a 2D PC waveguide structure that we discuss in this Letter. The waveguide has a finite wall thickness (each occupying N_w unit cells), and so wave leakage can happen for an otherwise perfectly confined guided wave. The optical properties of this waveguide can be characterized by three parameters, ω, k, and β.

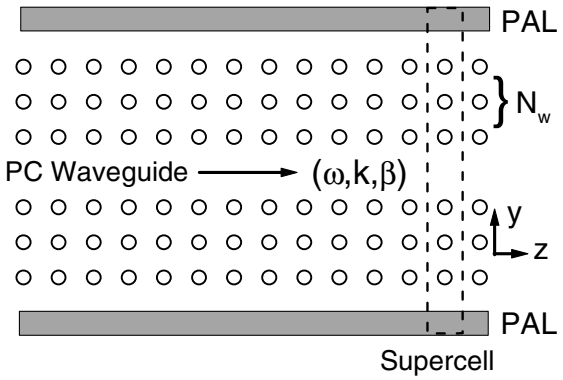

FIG. 1. Schematic configuration of light propagation in a 2D PC waveguide solved by the TMM approach. Two perfect absorption layers (PALs) are placed at the boundaries of the supercell to account for wave leakage.

In the TMM, the EM fields at the left and right hand sides of any supercell (denoted by a dashed rectangle in Fig. 1) are described by column vectors consisting of coefficients of forward and backward propagating plane waves as $\Omega_0 = (\Omega_0^+, \Omega_0^-)^T$ and $\Omega_1 = (\Omega_1^+, \Omega_1^-)^T$. It can be shown [15,16] that they are connected by a transfer matrix T,

$$\Omega_1 = T\Omega_0. \tag{1}$$

Because of the periodicity, the fields after traveling through n unit cells are given by

$$\Omega_n = T^n\Omega_0, \tag{2}$$

where $\Omega_n = (\Omega_n^+, \Omega_n^-)^T$. Obviously the unit-cell transfer matrix T plays a key role in determining the propagation behavior of the wave in the waveguide. To see this more clearly, suppose that Ω_0 is an eigenmode of T, and the corresponding eigenvalue is λ. From Eq. (2) we have

$$\Omega_n = \lambda^n\Omega_0. \tag{3}$$

The field is still an eigenmode of the waveguide, but witnesses a factor λ^n. For a truly guided mode in a PC waveguide with perfect confinement, λ is just the Bloch's phase factor $\lambda = e^{ikz}$ ($|\lambda| = 1$), and lossless propagation can be seen from Eq. (3). On the other hand, if $\lambda = e^{ikz-\beta z}$, where $\beta > 0$, one gets $|\lambda| < 1$. Then this corresponds to a decaying guided mode, and β is the decay constant for this mode. The above analysis has led to a simple yet elegant way to rigorously and quantitatively evaluate the propagation loss of a PC waveguide: Solve the transfer matrix T for a unit supercell of the PC waveguide system involving PALs at the boundaries, and pick up the decaying eigenmodes. Usually a lossy PC waveguide can support many decaying modes. The ways different decaying modes are excited by an external input wave can be investigated in the same TMM framework [16]. General speaking, the propagation loss of the waveguide is mainly determined by the least lossy mode with minimum decay constant β. A great advantage of this scheme is that the numerical burden does not have any dependence on the waveguide length.

Now we turn to the 2D PC waveguide displayed in Fig. 1. The background photonic crystal is made from a square lattice of dielectric cylinders with a lattice constant a, refractive index $n = 3.4$, and radius $r = 0.18a$ embedded in air. This crystal has a complete E-polarization band gap at frequencies [in units of $(2\pi c/a)$] from 0.302 to 0.443. The waveguide is created by removing a single row of cylinders along the (01) crystalline direction. A perfect waveguide with infinitely thick walls can support a single wide band of lossless guided modes. The band starts from a cutoff at $k = 0$ ($\omega = 0.312$) and extends straight upwards into the upper band edge. If the waveguide wall is not sufficiently thick, there will be a nonvanishing probability that the confined guided wave can tunnel through the walls and couple into the radiation modes in the air background, leading to propagation loss.

We first use a multiple scattering approach [17] similar to the familiar Korringa-Kohn-Rostoker (KKR) method to visualize the decay feature by looking at the field pattern along the waveguide axis at a certain excitation frequency. The waveguide is excited by an external E-polarized monochromatic point source placed in collimation to the waveguide axis. To see how the loss depends on the waveguide wall thickness, we have changed N_w from 1 to 5. Because of the limit of the computation source, the maximum waveguide length is 200 unit cells, and the maximum cylinder number is 2000 in our calculation.

Figure 2 displays several typical examples of the KKR simulation result for the field pattern along the waveguide axis. Three excitation frequencies 0.32, 0.37, and 0.43 are chosen, and they locate at the lower, middle, and upper parts of the guided-mode band (also the band gap), respectively. Several significant features can be found. First, the field profile can well be described by an exponential-decay function, a natural result when wave leakage occurs. For instance, for $N_w = 1$, the decay constant β (in units of a^{-1}) can be found by curve fitting to be 0.321, 0.0754, and 0.0038 at frequencies 0.32, 0.37, and 0.43, respectively. Second, the loss is reduced when the waveguide wall becomes thicker, also a natural result. For $N_w = 2$, β reduces to 0.071, 5.5×10^{-3}, and 9.2×10^{-4} at the three frequencies, while for $N_w = 3$, they become 0.0117, 3.9×10^{-4}, and 1.3×10^{-5}, respectively. Third, the loss is reduced when the frequency changes from the

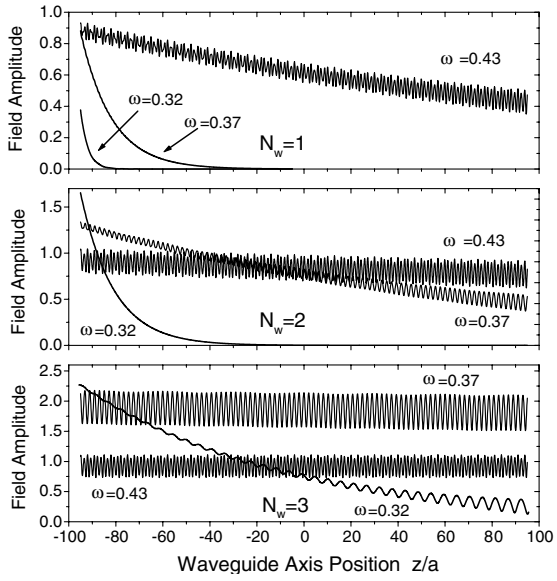

FIG. 2. KKR calculation results for the field pattern along the waveguide axis excited by an external monochromatic point source at different frequencies and different waveguide wall thicknesses.

lower end of the guided-mode band to the upper end. Finally, there exists remarkable interference in the waveguide induced by the reflection from the waveguide exit, especially in the low loss situations. Because of the interference, a single exponential-decay description of the field profile becomes less accurate, and this leads to some uncertainties in extracting the decay constant when it is in low level. This difficulty can be solved by adopting a much longer waveguide, for instance, a 5000 unit-cell long waveguide might be adequate to acquire the accurate decay constant value for $N_w = 3$ and $\omega = 0.43$. However, the numerical burden will become intolerable. Following the above procedures, we have been able to plot the overall decay picture for the whole guided-mode band at different wall thicknesses. This is summarized in Figs. 3(b) and 3(c) by solid circular dots. It is seen that β monotonically decreases with respect to both the excitation frequency and the wall thickness, both approximately following an exponential-decay law.

The difficulty induced by the rapidly growing numerical burden in the KKR simulation for a longer waveguide can be overcome by the above TMM. To facilitate the numerical stability and convergency, which is of vital importance for unambiguous extraction of the decay constant of an extremely low loss waveguide, we place special metallic plates at the supercell boundary to serve as PALs [18]. The permittivity ϵ of each metallic plate gradually increases from 1 at the inner surface (adjacent to air background) to $1 + 1.7i$ at the boundary. The plate is two unit cells thick in each supercell. This nearly adiabatic variation of ϵ can guarantee almost 100% absorption by the metal. For instance, EM waves at $\omega = 0.35$ normally incident on this metallic plate will witness a 0.5% reflection, 0.1% transmission, and 99.4% absorption. The metallic plate, indeed, can effectively prevent cross talk between adjacent supercells.

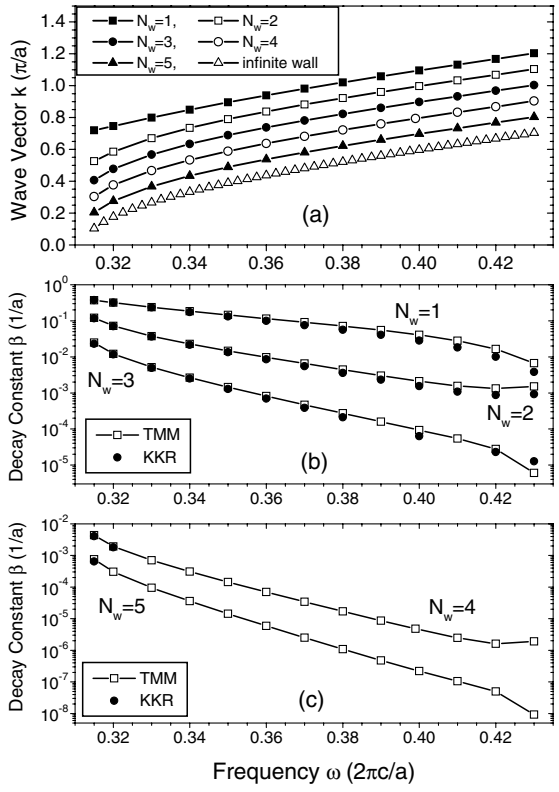

FIG. 3. (a) TMM calculation results of the dispersion for waveguides with different wall thicknesses. For the sake of easier viewing, the curves are offset alternately. (b),(c) Overall pictures for the propagation loss as a function of the excitation frequency and the waveguide wall thickness calculated by both the TMM and KKR approaches.

We have considered different waveguides with wall thicknesses from $N_w = 1$ to 5, and correspondingly supercell sizes of $9a$, $11a$, $13a$, $15a$, and $17a$ are adopted in the simulations. Eleven plane waves per unit cell are used, and good numerical convergence has been reached. The reason is that an optimum Fourier expansion rule has been available for the current problem concerning the E-polarization mode [15] even if metallic materials are involved in the structure. The calculation results for the decay constant as a function of the excitation frequency and the wall thickness are displayed in Figs. 3(b) and 3(c) by open square dots. The overall agreement with the KKR simulation results is excellent, indicating that the proposed TMM is quite efficient for this purpose of propagation loss solution. There is no difficulty in extracting reliable values of an extremely low loss (as small as 10^{-8}) in a waveguide with thick walls. This low loss level is beyond the scope of any other numerical approaches. Note that for a lossless waveguide, the calculated decay constant can be lower than 10^{-11}. The TMM can also yield the propagation wave vector k as a function of ω for a waveguide. This can be found in Fig. 3(a) for different wall thicknesses. As a reference, the dispersion for a perfect PC waveguide with infinitely thick walls is also shown. The dispersion of all waveguides with finite wall thickness almost resembles that of a perfect waveguide, indicating that the wave propagation behavior in these waveguides is close to that in a perfect waveguide. The only exception occurs at $N_w = 1$ and at $\omega < 0.36$, where appreciable deviation from the perfect-waveguide behavior is found. This is not hard to understand because this thin-wall waveguide can hardly be called a PC waveguide.

There are two significant points that one can find from the overall loss pictures shown in Fig. 3. First, the propagation loss essentially decays exponentially with respect to the cladding wall thickness of the waveguide. This phenomenon is not hard to understand, since within the band gap, the transmission is an exponential-decay function of the crystal thickness. The second thing turns out to be a surprising anomaly, where the propagation loss largely decays monotonously with respect to the excitation frequency, almost following an exponential-decay

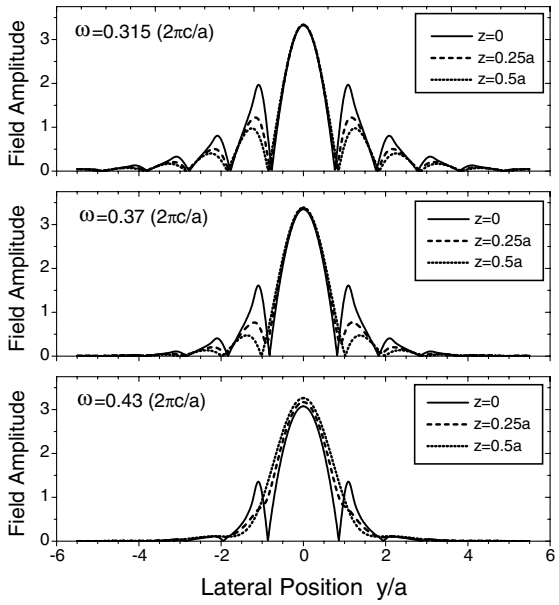

FIG. 4. Calculated field profile at three lines perpendicular to the waveguide axis at different frequencies. The line $z = 0$ passes through the center of cylinders.

law. The fact that the loss is far enhanced at the lower end of the guided-mode band (around the waveguide cutoff) is also not hard to understand because the group velocity here is much smaller than in other frequency domains. However, the observation that the loss around the upper-end region can be several orders of magnitude smaller than in the middle region of the band (also the center of the band gap) is not easy to swallow, as the group velocities are in almost the same level. In fact, the conventional wisdom holds that the wave attenuation through a photonic crystal slab should be maximum at the middle of the band gap, and this has been verified by many wave transmission experiments. Therefore, the wave leakage probability should be smaller here than in the two ends of the guided-mode band.

To understand the observed seemingly contradictory loss behavior, we look at the field profile of the guided-mode supported in a perfect PC waveguide. Figure 4 displays the results calculated by means of a plane-wave expansion method [19] along three lines perpendicular to the waveguide axis. The trend of increasing wave localization around the waveguide axis from lower frequencies to higher frequencies is obvious. As tighter localization means that the guided wave is subject to smaller influence when removing the outer shell of cylinders, it becomes harder and harder for the wave to leak out of the waveguide when ω increases from 0.315 to 0.37, and to 0.43. We believe that this surprising localization behavior is the main source behind the observed anomalous loss phenomena. This anomaly can provide a hint to design a low loss waveguide within a photonic crystal exhibiting a complete band gap but with limited cladding wall thickness due to, say, microfabrication difficulty. One can choose to operate the waveguide at a frequency domain near the upper band edge rather than in the middle of the band gap. We expect that this feature can also exist in a 3D photonic crystal waveguide [8].

In conclusion, we have employed a highly efficient TMM approach to investigate the propagation loss in a PC waveguide without complete wave confinement because of limited cladding wall thickness. As the numerical burden does not depend on the waveguide length, this method allows for accurate and reliable extraction of the propagation loss even at an extremely low level. An anomalous loss phenomenon is found where the loss for guided modes near the upper band edge can be several orders of magnitude smaller than that for modes in the middle of the band gap, and it is attributed to a different localization degree of the guided mode at different frequency domains. This feature can help to design a low loss PC waveguide.

Ames Laboratory is operated for the U.S. Department of Energy (DOE) by Iowa State University under Contract No. W-7405-Eng-82.

*Email address: lizy@axel.ameslab.gov

[1] E. Yablonovitch, Phys. Rev. Lett. **58**, 2059 (1987).
[2] J. D. Joannopoulos, P. R. Villeneuve, and S. Fan, Nature (London) **386**, 143 (1997).
[3] A. Mekis *et al.*, Phys. Rev. Lett. **77**, 3787 (1996); M. Bayindir *et al.*, Phys. Rev. B **63**, 081107 (2001); Z. Y. Li and K. M. Ho, J. Opt. Soc. Am. B **20**, 801 (2003).
[4] C. J. M. Smith *et al.*, Appl. Phys. Lett. **77**, 2813 (2000).
[5] M. Loncar *et al.*, Appl. Phys. Lett. **80**, 1689 (2002).
[6] T. Baba *et al.*, Electron. Lett. **37**, 761 (2001).
[7] M. Notomi *et al.*, IEEE J. Quantum Electron. **38**, 736 (2002).
[8] S. Y. Lin *et al.*, Nature (London) **394**, 251 (1998); S. Noda *et al.*, Science **289**, 604 (2000); C. Sell *et al.*, Phys. Rev. B **68**, 113106 (2003).
[9] T. Ochiai and K. Sakoda, Phys. Rev. B **63**, 125107 (2001).
[10] Y. Tanaka *et al.*, Appl. Phys. Lett. **82**, 1661 (2003).
[11] P. Paddon and J. F. Young, Phys. Rev. B **61**, 2090 (2000).
[12] L. C. Andreani, and M. Agio, Appl. Phys. Lett. **82**, 2011 (2003).
[13] R. Ferrini *et al.*, J. Opt. Soc. Am. B **20**, 469 (2003).
[14] A. Morand *et al.*, Opt. Commun. **221**, 353 (2003).
[15] Z. Y. Li and L. L. Lin, Phys. Rev. E **67**, 046607 (2003); L. L. Lin, Z. Y. Li, and K. M. Ho, J. Appl. Phys. **94**, 811 (2003).
[16] Z. Y. Li and K. M. Ho, Phys. Rev. B **68**, 155101 (2003).
[17] L. M. Li and Z. Q. Zhang, Phys. Rev. B **58**, 9587 (1998); Z. Y. Li and K. M. Ho, Phys. Rev. B **68**, 045201 (2003).
[18] E. Silberstein *et al.*, J. Opt. Soc. Am. A **18**, 2865 (2001).
[19] K. M. Ho, C. T. Chan, and C. M. Soukoulis, Phys. Rev. Lett. **65**, 3152 (1990); Z. Y. Li, J. Wang, and B. Y. Gu, Phys. Rev. B **58**, 3721 (1998).